⌘ *Author's Choice*

THE JOURNAL OF BIOLOGICAL CHEMISTRY VOL. 286, NO. 7, pp. 5404–5413, February 18, 2011

Reverse Engineering Gene Network Identifies New Dysferlin-interacting Proteins*[S]

Received for publication, August 10, 2010, and in revised form, November 29, 2010 Published, JBC Papers in Press, November 30, 2010, DOI 10.1074/jbc.M110.173559

Mafalda Cacciottolo[‡], Vincenzo Belcastro[‡], Steve Laval[§], Kate Bushby[§], Diego di Bernardo[‡], and Vincenzo Nigro[‡¶1]

From the [‡]TIGEM-Telethon Institute of Genetics and Medicine, 80131 Naples, Italy, the [§]Institute of Human Genetics, Newcastle University, NE1 3BZ Newcastle Upon Tyne, United Kingdom, and the [¶]Laboratorio di Genetica Medica, Dipartimento di Patologia Generale and CIRM, Seconda Università degli Studi di Napoli, 80138 Naples, Italy

Dysferlin (DYSF) is a type II transmembrane protein implicated in surface membrane repair of muscle. Mutations in dysferlin lead to Limb Girdle Muscular Dystrophy 2B (LGMD2B), Miyoshi Myopathy (MM), and Distal Myopathy with Anterior Tibialis onset (DMAT). The DYSF protein complex is not well understood, and only a few protein-binding partners have been identified thus far. To increase the set of interacting protein partners for DYSF we recovered a list of predicted interacting protein through a systems biology approach. The predictions are part of a "reverse-engineered" genome-wide human gene regulatory network obtained from experimental data by computational analysis. The reverse-engineering algorithm behind the analysis relates genes to each other based on changes in their expression patterns. DYSF and AHNAK were used to query the system and extract lists of potential interacting proteins. Among the 32 predictions the two genes share, we validated the physical interaction between DYSF protein with moesin (MSN) and polymerase I and transcript release factor (PTRF) in mouse heart lysate, thus identifying two novel Dysferlin-interacting proteins. Our strategy could be useful to clarify Dysferlin function in intracellular vesicles and its implication in muscle membrane resealing.

Dysferlinopathies are autosomal recessive muscle disorders caused by mutations in the Dysferlin (*DYSF*)[2] gene (1). Two major phenotypes have been described: Limb-Girdle Muscular Dystrophy type 2B (LGMD2B; OMIM253601) (2, 3) and Miyoshi myopathy (MM; OMIM254130). Dysferlin deficiency has also been associated with additional phenotypes such as Distal Myopathy with Anterior Tibial onset (DMAT, OMIM606768 (1)). Even if clinical differences should be, they may be not so striking at the molecular level (4). The *DYSF* gene is mainly expressed in skeletal and cardiac muscle as well as in monocytes/macrophages. It is localized to the plasma membrane of muscle fibers, but also to cytoplasmic vesicles (5, 6). Dysferlin is able to binds phospholipids in a Ca^{2+}-dependent manner through its C2-like domains, consistent with its role in skeletal muscle membrane repair. In the patch hypothesis for membrane repair proposed by Han and Campbell (5), Ca^{2+} flooding through a membrane disruption is thought to evoke local vesicle-vesicle and vesicle-plasma membrane fusion events. As a result, a population of large vesicles accumulates underneath the disruption site, eventually creating a patch of new membrane across the membrane gap via vesicle-vesicle and vesicle-membrane fusion. This function is also supported by ultrastructural observations of dysferlin-deficient skeletal muscle: subsarcolemmal regions are characterized by prominent aggregations of small vesicles of unknown origin. In the past, many research groups have carried out studies to find new Dysferlin-interacting proteins to clarify the pathway in which Dysferlin is involved and investigate its function. Different approaches have been used for that purpose, such as proteomics analysis (ANNEXINS (7), AHNAK (8), α-tubulin (9)), and screening on muscle samples from patients (caveolin 3 (10), Calpain3 (11); DHPR (12), AFFIXIN (13)). Systems biology is emerging as a revolutionary approach to the analysis of mechanisms underlying protein function (14), acquiring information from the huge amount of data collected in public databases, in particular the increasing number of microarray studies in both patients and animal models with mutations in a variety of different muscular dystrophy-associated genes (15–18). These studies have identified some secondary changes, which appear to be common to muscular dystrophy in general. The compilation of particular expression profiles from patients and animal models of specific types of muscular dystrophy may eventually delineate a reproducible "molecular signature" of disease. These studies produced a lot of information about the possible changes occurring in dysferlinopathy, but the analysis of any single study is subject to error. "Reverse-engineering" programs allow an effective meta-analysis of multiple studies. Here we show the power of a "reverse-engineering" gene network to identify new interacting proteins. Using a new algorithm developed in our institute, we identified and experimentally confirmed the interaction between DYSF and MSN and PTRF.

* This study was supported by grants from Telethon (TIGEM-TNP42TELC) and FP7/2007-2013 under Grant agreement no. 223143 (Project acronym: TECHGENE), from Ministero della Salute (Ricerca Finalizzata RF-MUL-2007-666195) and from Telethon-UILDM.

⌘ *Author's Choice*—Final version full access.

[S] The on-line version of this article (available at http://www.jbc.org) contains supplemental Table S1.

[1] To whom correspondence should be addressed: Telethon Institute of Genetics and Medicine (TIGEM), Via Pietro Castellino 111, 80131 Napoli and Dipartimento di Patologia Generale, Seconda Università degli Studi di Napoli, S. Andrea delle Dame, via L. De Crecchio 7, 80138 Napoli, Italy. Tel./Fax: 39-0815665704; E-mail: vincenzo.nigro@unina2.it or nigro@tigem.it.

[2] The abbreviations used are: DYSF, Dysferlin; LGMD, limb-girdle muscular dystrophy; MM, Miyoshy Myopathy; DMAT, distal myopathy with anterior tibial onset; MSN, moesin; GSN, gelsolin; PTRF, polymerase I and transcript release factor; MI, mutual information.

EXPERIMENTAL PROCEDURES

Bioinformatic Analysis—Netview[3] is a web tool that collects predictions on genetic regulatory influences. A pair-wise score between each pair of human genes was computed from their expression profiles. The program examined the data and discriminated between the Affymetrix ID, which mRNA was contemporaneously or not up- or down-regulated and which was the more significant variation compared with variation of a query. In particular, the mutual information (MI) between each pair of genes was computed and stored in a database. MI can be seen as a correlation among the expression profiles of the two genes. However, as they showed, MI is more general and powerful than correlation. MI measures how coherently the expression of a gene pair varies together. Expression profiles were downloaded form Array Express (19), a large repository of expression data. More that 20,000 hybridization, from 614 different experiments, were used to reverse-engineer the human gene regulatory network. MI has been widely applied to infer gene networks (20, 21). The network was cleaned for false positives by applying a Data Process Inequality step as previously described (22). All the results are collected and accessible upon registration.

Animals—Both Dysferlin-deficient C57BL/10.SJL-Dysf (23) and B6.129-Dysf^{tm1Kcam}/Mmmh (24) (produced in Campbell's laboratory, further indicated as Camp mouse) were used for this study. All strains of mice were housed under standard conditions and used according to the Animal Procedures Committee, Home Office, UK and local rules. Heart and skeletal muscles were collected from old diseased and control mice and used for the WB analysis.

Cell Culture—The African Green Monkey SV40 transformed kidney fibroblast cell line, COS7 cells were purchased from ATCC (Burlington, Ontario; ATCC number CRL-1573). The cells were grown in Dulbecco's modified Eagle's medium (Invitrogen, Carlsbad, CA) containing 10% fetal bovine serum. Cells were transfected according to the Polifect manufactures instruction (Qiagen GmbH, Hilden, Germany).

Plasmid Constructs—The GFP-His-Myc-tagged dysferlin cDNA cloned into DSC-B plasmid was previously described (25). In this construct, the GFP coding sequence is located at the 5′-end, and the His-Myc tags are located at the 3′-end of the dysferlin cDNA. The MSN and PTRF constructs were generated from common PCR amplification using human healthy patient cDNA(MSN_1F_EcoRI_CCGGAATTCAACATGCCCAAAACGATCAG,MSN_1734R_XhoI CCGCTCGAGTGCCCATTACATAGACTC,PTRF_1F_EcoRI_CCGGAATTCGCCATGGAGGACCCCACGCTC, PTRF_1173R_BamHI_GCGGATCCCGGCTCAGTCGCTGTCGCT). Appropriate restriction sites were included in the primer sequence to facilitate subcloning of the PCR fragments into pcDNA3-HA (Invitrogen).

Selection of Patients—Different exemplary patient biopsies were selected for this study and both clinically and genetically classified by molecular analysis of both DNA and RNA samples. Three anonymous patients were affected by LGMD2B, one by LGMD2A, one by LGMD2C, and last one by BMD (see Table 1). Two control biopsies from healthy subjects were included in the study.

Preparation of Muscle Extracts and Western Blot Analysis—Muscle extracts were collected from patient muscle biopsies and both skeletal muscle and heart of dysferlin-deficient mouse models and controls. Muscle samples were homogenized in RIPA buffer (10 mM Tris, pH 7.4, 150 mM NaCl, 0.2% Triton X-100, 2 mM EDTA, 1 mM PMSF, and 1× Protease Inhibitor Mixture). 10 μg of total protein were resolved by SDS-PAGE and transferred to a nitrocellulose membrane. Antibody dilutions were 1:300 anti-Dysferlin (DYSF, Hamlet, Novocastra), 1:5000 anti-moesin (MSN, BD Bioscience), 1 μg/ml anti-gelsolin (GSN, Abcam), 0.625 μg/ml anti-PTRF (Abcam), 1:10000 anti GAPDH (SantaCruz Biotechnology). After washing, horseradish peroxidase-conjugated anti-mouse or anti-rabbit antibody was used to visualize bound primary antibodies with the ECL chemiluminescence system (Supersignal, WestPico, Pierce).

Immunofluorescence Assay—COS7 cells were grown on glass coverslips in 6-well plates (NUNC A/S, Roskilde, Denmark). They were cultured in Dulbecco's modified Eagle's medium (DMEM) supplemented with 10% (v/v) fetal bovine serum and penicillin-streptomycin (Invitrogen) and maintained in a 5% CO_2 incubator at 37 °C. Transfections were carried out using Polyfect reagent (Invitrogen) according to the manufacturer's protocol. After 36 h, cells were fixed in 4% paraformaldehyde/PBS for 10 min at room temperature. An antibody against the HA epitope (monoclonal from Roche; polyclonal from Sigma) was used to detect MSN and PTRF constructs, while Dysferlin expression was followed by EGFP fluorescence. Cy3-conjugated anti-mouse and Fitch-conjugated anti-rabbit secondary antibodies were used. Coverslips were mounted using Vectashield mounting medium with DAPI (Vector Laboratories Inc., Burlingame, CA). Cells were examined using a Zeiss microscope (Axio Imager A1, Carl Zeiss S.p.A, Milan, Italy) and analyzed using Axio Vision Rel. 4.5 software. Digital images were saved and managed by Adobe PhotoShop (Adobe Systems Inc., Mountain View, CA).

For immunofluorescence on muscle sections, 7 μm slides were used and tested for the expression of Dysferlin and PTRF using specific antibodies following the protocol previously described (26). The working dilution were: Dysferlin (NCL-Hamlet) 1:20, PTRF (Abcam) 1:100. As a negative control, the secondary antibodies alone were used.

Immunoprecipitation of Mouse Heart Samples—Heart tissue from a wt mouse was homogenized in RIPA buffer containing 10 mM Tris, pH 7.4, 150 mM NaCl, 0.2% Triton X-100, 2 mM EDTA, 1 mM PMSF, and 1× Protease Inhibitor Mixture (Complete Tablets, Roche). Muscle heart lysate was centrifuged at 14,000 rpm for 10 min at 4 °C, and the supernatant collected. 500 μg of total protein was pre-cleared by addition of 250 μl of 1:1 slurry of protein A (Roche) washed and resuspended in PBS. After 30 min at 4 °C, samples were centrifuged for 10 min at 14,000 rpm. The resulting supernatants were transferred to fresh tubes, and 20 μl of monoclonal anti-Dysferlin antibody (Hamlet, NCL) was added and incubated ON at 4 °C. After incubation, 80 μl of 1:1 slurry of Protein

[3] V. Belcastro, F. Iorio, and D. di Bernardo, under review.

A-Sepharose were added to each sample, and the mixture of lysate and beads was incubated for 4 h at 4 °C. Immunoprecipitates were then washed 3 times with lysis buffer, and analyzed by WB with specific primary antibodies.

Muscle Fractionation—Skeletal muscles from wild-type and SJL mice were collected and homogenized in 0.25 M sucrose, 1 mM EDTA, 20 mM HEPES-KOH, pH 7.4) using TissueRuptor (Qiagen) at 4 °C. To achieve the best resolution and recovery of a specific subcellular particle, a fixed-angle rotor was used for all differential centrifugation. The sample was pelleted by centrifuging the total lysate at 10,000 rpm for 15 min at 4 °C in a fixed-angle rotor. Supernatant medium was collected and filtered through four layers of gauze to remove any particulate material and connective tissue still in solution. The resulting sample was layered onto a linear 10–50% sucrose-optiprep density gradient and subjected to ultracentrifugation (Sw41Ti rotor, 27,000 rpm for 4 h at 4 °C). The gradient was then fractionated; the fractions were collected analyzed by WB.

RESULTS

Identification of Potential DYSF-interacting Proteins—The results of the reverse-engineering[3] analysis were collected in a database available on the Web. The rationale behind this approach is that genes, coherently expressed in a large set of hybridization, may share a common regulator (27), may be influencing each other or may be involved in the same pathway. To extract new potential DYSF interactions, and to gain new information about the correlation between genes in LGMDs, we ran the program for all the LGMDs genes, and produced evidence of gene clustering in many cases. Multiple runs of Netview suggested that for most LGMD genes no correlation was evident. In contrast, dysferlin clustered together with the genes belonging to the membrane repair group, such as ANNEXIN, AHNAK. Because AHNAK is a protein that is considered to be a DYSF-interacting partner (8) and their likely subcellular localization implicates the AHNAK-Dysferlin complex in membrane repair, we looked at the intersection of the dysferlin and AHNAK networks to identify the membrane repair complex. We used DYSF and AHNAK for further analysis. The system has been asked to retrieve all the genes, within the human network, predicted to be directly connected to DYSF. A direct connection between two genes exists whenever their MI is statistically significant (20, 22). The output of the queries consists of two sub-networks of the human network surrounding the genes of interest. All of the genes, that are predicted to be connected at the gene of interest, are definitively co-expressed with the gene of interest in most of the analyzed hybridizations. Querying the system with DYSF identified a series of genes, among these were known Dysferlin-interacting proteins such as CD14, important markers for the isolation of Dysferlin-positive macrophage, Annexin and S100A family proteins. A number of similar interactions were also recognized in the analysis of ANHAK, such as Annexin and the S100A. Results are shown in Tables 1 (DYSF analysis) and Tables 2 (AHNAK analysis). In Tables 1 and 2, some gene was considered more than once. This happened because the "human gene network" we infer in reality is a "human probe network." There are probes in the HG-U133A platform that refer to the same gene, but the expression profiles of those probes are far from being correlated. Many reasons drive such behavior, *i.e.* wrong probe design, multiple gene splicing, etc. For these reasons we decided to keep all the probes and infer a probe-wise human network.

TABLE 1
Results of reverse-engineering analysis using the *DYSF* gene

Probeset ID	Gene symbol	MI	Probeset ID	Gene Symbol	MI
205119_s_at	FPR1	0.0506	201743_at	CD14	0.0339
211133_x_at	LILRA6 /// LILRB3	0.0494	204204_at	SLC31A2	0.0339
211135_x_at	LILRB3	0.0488	201785_at	RNASE1	0.0336
204232_at	FCER1G	0.0477	204122_at	TYROBP	0.0335
209791_at	PADI2	0.0467	222218_s_at	PILRA	0.0335
210784_x_at	LILRA6 /// LILRB3	0.0459	211582_x_at	LST1	0.0332
208018_s_at	HCK	0.0456	210184_at	ITGAX	0.033
205237_at	FCN1	0.0452	203591_s_at	CSF3R	0.0329
213733_at	MYO1F	0.0449	210785_s_at	C1orf38	0.0328
202878_s_at	CD93	0.0446	202510_s_at	TNFAIP2	0.0327
204007_at	FCGR3B	0.0424	205142_x_at	ABCD1	0.0327
205936_s_at	HK3	0.0421	206380_s_at	CFP	0.0326
210225_x_at	LILRB3	0.0414	209906_at	C3AR1	0.0325
202877_s_at	CD93	0.0403	205147_x_at	NCF4	0.0324
211100_x_at	LILRA2	0.0403	214181_x_at	LST1	0.0322
202803_s_at	ITGB2	0.04	203104_at	CSF1R	0.0321
204436_at	PLEKHO2	0.0396	205098_at	CCR1	0.032
207571_x_at	C1orf38	0.0392	215633_x_at	LST1	0.0319
38487_at	STAB1	0.0389	202637_s_at	ICAM1	0.0318
211581_x_at	LST1	0.0382	203167_at	TIMP2	0.0318
203175_at	RHOG	0.038	203936_s_at	MMP9	0.0316
38671_at	PLXND1	0.0378	209949_at	NCF2	0.0316
208594_x_at	LILRA6	0.0377	213592_at	AGTRL1	0.0316
208981_at	PECAM1	0.037	209933_s_at	CD300A	0.0315
204150_at	STAB1	0.0369	202974_at	MPP1	0.0314
205786_s_at	ITGAM	0.0368	209473_at	ENTPD1	0.0312
38964_r_at	WAS	0.0365	214438_at	HLX	0.0312
210423_s_at	SLC11A1	0.0363	221060_s_at	TLR4	0.0312
203535_at	S100A9	0.0361	204959_at	MNDA	0.031
214511_x_at	FCGR1B	0.0361	210146_x_at	LILRB2	0.0309
210629_x_at	LST1	0.036	216950_s_at	FCGR1A	0.0309
207697_x_at	LILRB2	0.0359	220088_at	C5AR1	0.0309
202897_at	SIRPA	0.0358	204265_s_at	GPSM3	0.0308
205568_at	AQP9	0.0358	205247_at	NOTCH4	0.0308
44673_at	SIGLEC1	0.0356	219183_s_at	PSCD4	0.0308
211101_x_at	LILRA2	0.0356	203761_at	SLA	0.0306
203508_at	TNFRSF1B	0.0353	64064_at	GIMAP5	0.0305
214574_x_at	LST1	0.0351	204043_at	TCN2	0.0305
205863_at	S100A12	0.035	204858_s_at	TYMP	0.0305
210845_s_at	PLAUR	0.0348	211433_x_at	KIAA1539	0.0305
208438_s_at	FGR	0.0347	203470_s_at	PLEK	0.0304
219666_at	MS4A6A	0.0346	215706_x_at	ZYX	0.0304
202896_s_at	SIRPA	0.0345	205986_at	AATK	0.0303
221541_at	CRISPLD2	0.0345	213095_x_at	AIF1	0.0303
211336_x_at	LILRB1	0.0344	210644_s_at	LAIR1	0.0302
205418_at	FES	0.0342	201042_at	TGM2	0.0301
208092_s_at	FAM49A	0.0342	212974_at	DENND3	0.0301
211661_x_at	PTAFR	0.0341			

Selection of Possible Candidates—We were interested in identifying proteins co-regulated and therefore potentially interacting with both DYSF and AHNAK. This removed all the genes that were predicted to connect with only either DYSF or AHNAK. The remaining 32 genes are highlighted in Table 3. Some top ranked genes have not previously been associated with muscle function, thus we decided to exclude them as muscle candidates. Thus GSN, MSN, PTRF were further analyzed.

Protein Expression Analysis on Mouse and Patients Samples—To investigate whether there is a co-regulatory relationship between Dysferlin and these candidates at the protein level, we performed an expression analysis by WB using Dysferlin-deficient mouse tissues. 10 μg of muscle lysate was loaded on a SDS-Page and tested for the expression of all candidates. All proteins showed no significant difference in ex-

TABLE 2

Results of reverse-engineering analysis using the Ahnak gene

Probeset ID	Gene Symbol	MI	Probeset ID	Gene symbol	MI
210427_x_at	ANXA2	0.0553	200911_s_at	TACC1	0.0352
213503_x_at	ANXA2	0.0552	216264_s_at	LAMB2	0.0352
201590_x_at	ANXA2	0.0544	210840_s_at	IQGAP1	0.0349
200872_at	S100A10	0.0529	221718_s_at	AKAP13	0.0347
200791_s_at	IQGAP1	0.05	209341_s_at	IKBKB	0.0346
208634_s_at	MACF1	0.0489	201057_s_at	GOLGB1	0.034
200859_x_at	FLNA	0.0487	208633_s_at	MACF1	0.034
212586_at	CAST	0.0481	57715_at	FAM26B	0.0339
212377_s_at	NOTCH2	0.047	201394_s_at	RBM5	0.0339
212086_x_at	LMNA	0.0469	208763_s_at	TSC22D3	0.0339
201426_s_at	VIM	0.0467	202180_s_at	MVP	0.0335
208816_x_at	ANXA2P2	0.0466	220974_x_at	SFXN3	0.0335
214752_x_at	FLNA	0.0463	208789_at	PTRF	0.0333
214722_at	NOTCH2NL	0.0459	201087_at	PXN	0.0332
208683_at	CAPN2	0.0458	201368_at	ZFP36L2	0.0331
203411_s_at	LMNA	0.0455	211452_x_at	LRRFIP1	0.033
220016_at	AHNAK	0.0455	201009_s_at	TXNIP	0.0329
205081_at	CRIP1	0.0452	202378_s_at	LEPROT	0.0324
201029_s_at	CD99	0.0451	201103_x_at	KIAA1245	0.0322
221725_at	—	0.0445	201887_at	IL13RA1	0.0322
201778_s_at	KIAA0494	0.0434	201105_at	LGALS1	0.0318
219371_s_at	KLF2	0.0428	211864_s_at	FER1L3	0.0318
200696_s_at	GSN	0.0425	33850_at	MAP4	0.0317
201012_at	ANXA1	0.0425	201862_s_at	LRRFIP1	0.0317
217730_at	TMBIM1	0.0424	206200_s_at	ANXA11	0.0317
201798_s_at	FER1L3	0.0421	213612_x_at	KIAA1245	0.0317
202443_x_at	NOTCH2	0.0418	215235_at	SPTAN1	0.0317
203445_s_at	CTDSP2	0.0412	200907_s_at	PALLD	0.0316
202808_at	C10orf26	0.0405	217728_at	S100A6	0.0314
201010_s_at	TXNIP	0.0398	201412_at	LRP10	0.0313
201028_s_at	CD99	0.0396	200760_s_at	ARL6IP5	0.0312
212089_at	LMNA	0.0395	212566_at	MAP4	0.0312
213746_s_at	FLNA	0.0395	202117_at	ARHGAP1	0.0308
218204_s_at	FYCO1	0.039	212195_at	IL6ST	0.0308
208961_s_at	KLF6	0.0387	200804_at	TEGT	0.0307
219563_at	C14orf139	0.0386	214924_s_at	TRAK1	0.0307
208944_at	TGFBR2	0.0383	202771_at	FAM38A	0.0306
213656_s_at	KLC1	0.0382	207761_s_at	METTL7A	0.0306
217795_s_at	TMEM43	0.0379	217523_at	CD44	0.0306
212063_at	CD44	0.0377	200761_s_at	ARL6IP5	0.0305
201648_at	JAK1	0.0375	201324_at	EMP1	0.0305
201331_s_at	STAT6	0.0372	212914_at	CBX7	0.0305
217844_at	CTDSP1	0.0372	201302_at	ANXA4	0.0304
208614_s_at	FLNB	0.0367	213364_s_at	SNX1	0.0304
200797_s_at	MCL1	0.0365	203380_x_at	SFRS5	0.0303
214736_s_at	ADD1	0.0363	212567_s_at	MAP4	0.0302
201373_at	PLEC1	0.036	219165_at	PDLIM2	0.0302
203186_s_at	S100A4	0.0356	201552_at	LAMP1	0.0301
203729_at	EMP3	0.0356	201861_s_at	LRRFIP1	0.0301
211926_s_at	MYH9	0.0356	208908_s_at	CAST	0.0301

TABLE 3

Results of reverse-engineering analysis common to both AHNAK and the Dysferlin gene

For all probes we selected the top 1,000 MI; we merged the MI for both ANHAK probes and then we considered only the highest MI (when two probes represent the same transcript). Then we considered the intersection of two sets (AHNAK plus DYSF) thus obtaining the shared genes. In the case of multiple probes, the highest MI was only considered.

Gene name	Chr. localization	Ahnak score	Dysf score	Affimetrix ID
A2M	chr12p13.3-p12.3	6.86E+02	4.44E-03	217757_at
BCL6	chr3q27	9.87E+02	4.60E+02	203140_at
CD93	Chr20p11.21	5.60E+02	4.60E+02	202878_s_at
CD97	Chr19p13	7.12E+02	7.07E+00	202910_s_at
CDH5	Chr16q22.1	1.34E+02	2.92E-02	204677_at
COL8A2	Chr1p34.2	8.86E+01	1.86E+02	221900_at
CRISPLD2	Chr16q24.1	9.53E-04	8.41E-07	221541_at
EHD2	Chr19q13.3	2.38E-01	6.04E+00	45297_at
F13A1	chr6p25.3-p24.3	7.89E+02	4.14E-01	203305_at
FAM26B	chr10pter-q26.12	1.04E-05	8.73E+00	57715_at
FCGRT	Chr19q13.3	4.76E+01	2.62E+02	218831_s_at
FGL2	Chr7q11.23	2.49E-03	3.23E-02	204834_at
GIMAP6	Chr7q36.1	3.10E+02	1.21E+02	219777_at
GRN	Chr17q21.32	7.93E+02	2.63E+02	216041_x_at
GSN	chr9q33	0.000000e+00	3.32E-02	200696_s_at
KCTD12	Chr13q22.3	2.19E-01	2.25E+01	212192_at
MXRA8	Chr1p36.33	9.83E+01	2.59E+01	213422_s_at
LRP1	chr12q13-q14	3.19E+02	9.32E+01	200785_s_at
MSN	chrXq11.2-q12	1.15E+00	3.94E+02	200600_at
PDLIM2	Chr8p21.2	1.05E-02	5.87E+02	219165_at
PEA15	Chr1q21.1	3.48E+00	3.58E+02	200788_s_at
PECAM1	Chr17q23	3.99E+01	0.000000e+00	208983_s_at
PLXND1	Chr3q21.3	6.30E-01	5.52E-02	38671_at
PTRF	Chr17q21.31	0.000000e+00	1.21E+02	208789_at
RHOB	chr2p24	1.45E+02	6.42E+02	212099_at
SASH1	chr6q24.3	2.80E+01	3.73E+02	213236_at
STAB1	chr3p21.1	4.76E+00	6,41E-05	204150_at
TLR5	chr1q41-q42	2.79E+02	2.14E+00	210166_at
TNFSF12	Chr17p13.1	4.32E+02	3.05E+01	209499_x_at
TNFSF13	Chr17p13.1	4.75E+02	4.56E+02	210314_x_at
TNS1	chr2q35-q36	5.54E-02	5.65E+02	221748_s_at
VCAN	chr5q14.3	2.19E+01	3.32E-03	204620_s_at

pression between wt and diseased muscles, but strongest bands were observed in heart samples compared with the skeletal muscle from TA (Fig. 1*a*).

To investigate the role of candidates in LGMDs we tested the expression of the same antibodies on human protein samples of clinically and genetically classified patients. The clinical features of the patients and the causative mutations are summarized in supplemental Table S1. At the histological level, all the patients displayed severe variability in muscle fiber size, degenerating/regenerating fibers with an increased number of central nuclei, and an increase in connective tissue. 10 μg of each samples were analyzed by Western blotting, normalized to GAPDH expression. As shown in Fig. 1*B*, no significant differences were observed for GSN, while PTRF and MSN showed increased expression of PTRF and MSN was observed in LGMD patients compared with BMD and control samples.

IF Assay to Determine the Subcellular Localization—To gain information about the subcellular localization and validate any potential interaction, human MSN and PTRF coding sequence were cloned into the eukaryotic expression vector pcDNA3-HA and transfected into COS7 cells alone and in association with Myc-EGFP-DFL construct. First, we tested the efficacy of transfection using the single construct. PTRF and MSN were followed using the polyclonal antibody against HA epitope, while DYSF through the monoclonal anti-Myc antibody. Both proteins showed both cytoplasmatic and submembrane expression (Fig. 2, *a–f*). Then, we co-transfected both construct and followed DYSF by the GFP while MSN and PTRF using the monoclonal antibody for the HA epitope. IF staining (Fig. 2, *g–k*) showed a perfect merge of Dysferlin with both MSN and PTRF. The signal was observed both in the cytoplasm and along the plasma membrane (Fig. 2, *a–k*). We previously described the use of skin biopsies to analyze muscle proteins and obtain information about their subcellular localization in dystrophic as well as control samples (26). So, to get more evidence of a co-localization of Dysferlin and both PTRF and MSN, we performed an immunofluorescence assay on both a skin biopsy taken from a normal control (Fig. 3*a*) and muscle sections from a wild type mouse (Fig. 3*b*). As seen in Fig. 3, *a* and *b*, the proteins show a common pattern of expression of sarcolemmal staining in common with many muscle proteins. The IF assay, on both cells and tissues samples, is consistent with a possible interaction of DYSF with MSN and PTRF. To determine whether the absence of dysferlin affected PTRF localization, we performed immunofluorescence on muscle samples from an LGMD2B patient (Fig. 3*c*) and Camp mouse (Fig. 3*d*). As shown in Fig. 3, *c* and *d*, the absence of dysferlin did not alter the staining pattern of PTRF, which

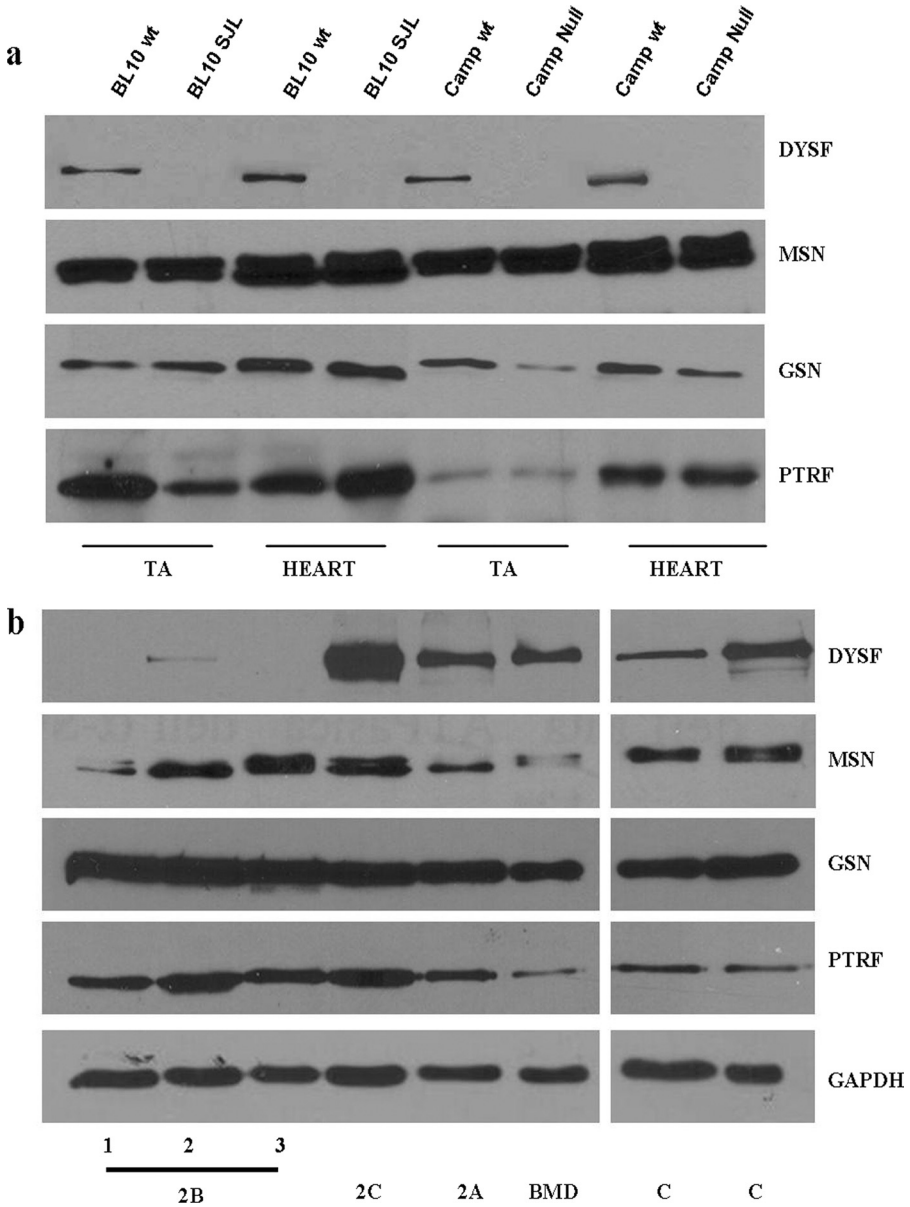

FIGURE 1. **Expression level of MSN, GSN, and PTRF in dysferlin deficient mice and LGMD2B patients.** Muscle extracts were collected from both the tibialis anterior and heart muscle of dysferlin-deficient mouse models (*a*), patient muscle biopsies (*b*), and controls. Muscle samples were homogenized in RIPA buffer. An equal amount of protein was separated on SDS-PAGE gels. Transferred immunoblots were probed for the relative expression levels of DYSF, MSN, GSN, and PTRF. *BL10-wt* are wild type BL10 mice; *BL10-SJL* are Dysferlin-deficient strain; *Camp-wt* are wild type B6.129; *Camp-null* are B6.129-Dysf^{tm1Kcam}/Mmmh. The results are representative of at least three independent experiments.

resembles the control in both mouse and patient tissues. As a negative control, the secondary antibodies alone were used (data not shown).

In Vivo Validation of Interaction—To verify whether DYSF associates directly with the selected proteins, we performed an immunoprecipitation experiment using both cellular lysate (for MSN, data not shown) and tissue. First of all, we tested the expression of candidates by specific antibodies on both cell lines and muscles (data not shown).

Because of high expression of candidates in heart muscle (Fig. 1*a*), immunoprecipitation assay was performed on mouse heart lysate. Heart lysates from wt and Camp mouse were incubated with anti-Dysferlin antibody and after washing the immunoprecipitated protein sample was tested for the presence of selected proteins (Fig. 4*a*). A lysate from a healthy subject was introduced as an additional positive control, to clarify the nature of positive bands. As shown in the Fig. 4*a*, positive bands were obtained for MSN and PTRF, but not for GSN in IP samples. Negative controls were introduced: we tested the same samples with (i) the secondary antibody alone to exclude the unspecific reaction, (ii) an unrelated antibody (for β-dystroglycan, βDG) and (iii) the IP on tissue from Dysferlin-deficient mice.

Additionally we performed another immunoprecipitation assay using both the PTRF and the MSN antibodies to immunoprecipitate the same heart lysate. As showed in Fig. 4, *b* and *c*, both the PTRF and the MSN antibodies were able to immunoprecipitate Dysferlin confirming the interaction.

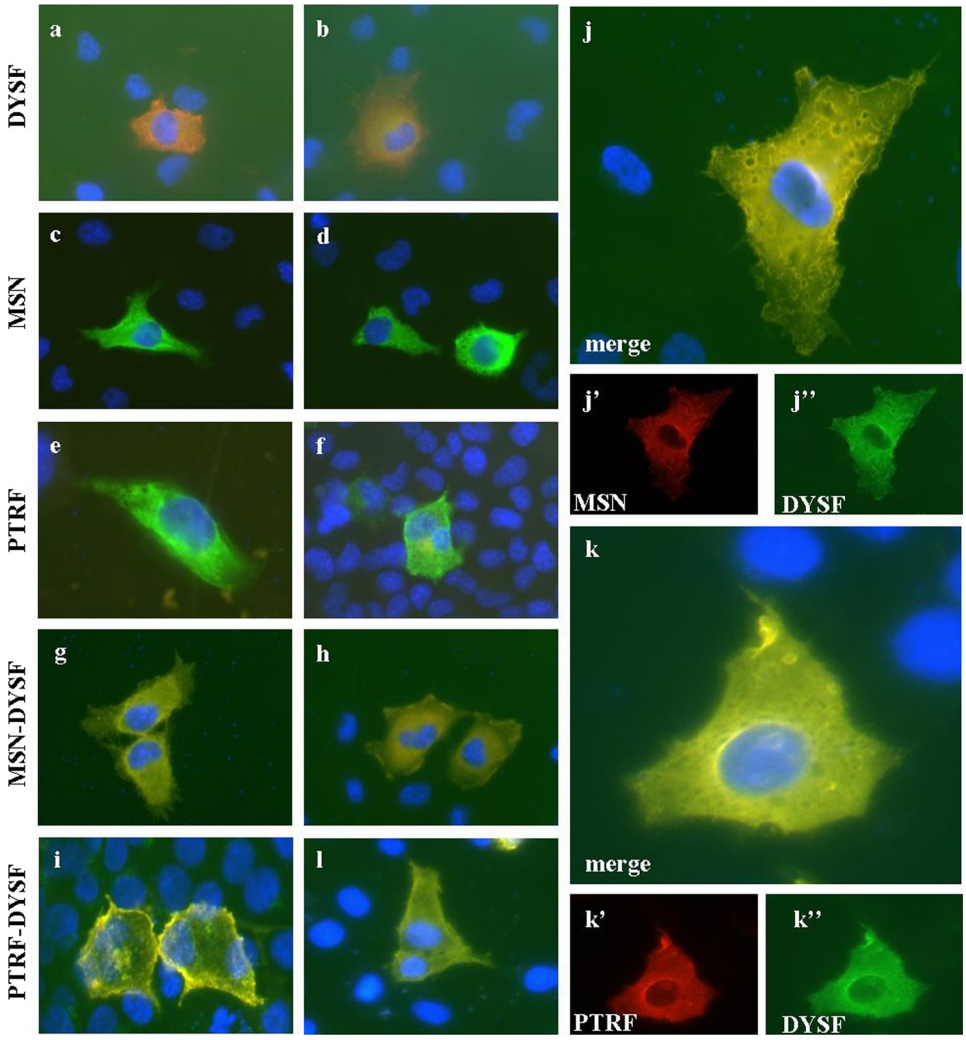

FIGURE 2. **Dysferlin co-localizes with MSN and PTRF.** COS7 cells were grown on glass coverslips in 6-well plates and transfected with the specific construct. After 36 h, cells were fixed in 4% paraformaldehyde/PBS for 10 min at room temperature. *a* and *b*, COS7 cells were transfected with Myc-Dysferlin alone and followed by a monoclonal anti-Myc antibody. *c–f*, COS7 cells were transfected with MSN construct (*c* and *d*) or PTRF (*e* and *f*) alone followed by a polyclonal anti-Ha antibody. *g–l*, COS7 cell were transfected with EGFP-DYSF construct together with HA-MSN (*g*, *h*, *k*) or HA-PTRF (*i*, *j*, *l*). An antibody against the HA epitope was used to detect MSN and PTRF constructs, while Dysferlin expression was followed by EGFP fluorescence. The results are representative of at least three independent experiments.

Subfractionation of Muscle Lysate—Because of the evidence of an intracellular vesicular localization of both PTRF (28) and DYSF (5, 7, 29) and their relationship to CAV3 (28, 30), we decided to analyze the distribution of both proteins in a linear gradient. Muscles collected from wt mouse lower limbs were homogenized with a 0.25 M sucrose solution to disrupt cellular but not vesicle membrane and centrifuged to obtain a microsomal sample, enriched in intracellular vesicles. This sample was loaded on a density gradient and centrifuged to allow the sample to equilibrate in the density gradient with the consequent separation of vesicles by buoyant density. Thirty fractions were collected from the gradient starting from the top and analyzed for the expression of DYSF, CAV3, as a positive marker, and PTRF through Western blot. As shown in Fig. 5, Dysferlin-positive vesicles concentrated in the middle part of the gradient. Most of fractions with an intense Dysferlin signal also showed a strong signal for caveolin3, a known Dysferlin-interacting protein, identifying the correct vesicle compartment. We observed that the same fractions were also positive for the expression of PTRF protein, supporting the hypothesis of a physical interaction and localization in the same vesicle compartment consistent with a common function in the muscle fiber.

To determine whether the absence of Dysferlin affects vesicle formation and/or the localization along the density gradient, we collected the muscles from 6 month old Camp mice and performed the sedimentation assay. The thirty fractions were tested for the expression of DYSF, CAV3, and PTRF. As expected, the fractions were negative for Dysferlin (Fig. 5), while PTRF and CAV3 showed a strong staining, with a slight shift to the bottom of the gradient. Increased presence of PTRF and Cav3-positive vesicles may reflect the increased vesicles numbers observed in many studies on dysferlinopathic muscles (5).

DISCUSSION

LGMDs are genetically heterogeneous despite similar phenotypes (31). Primary defects involve different cellular pro-

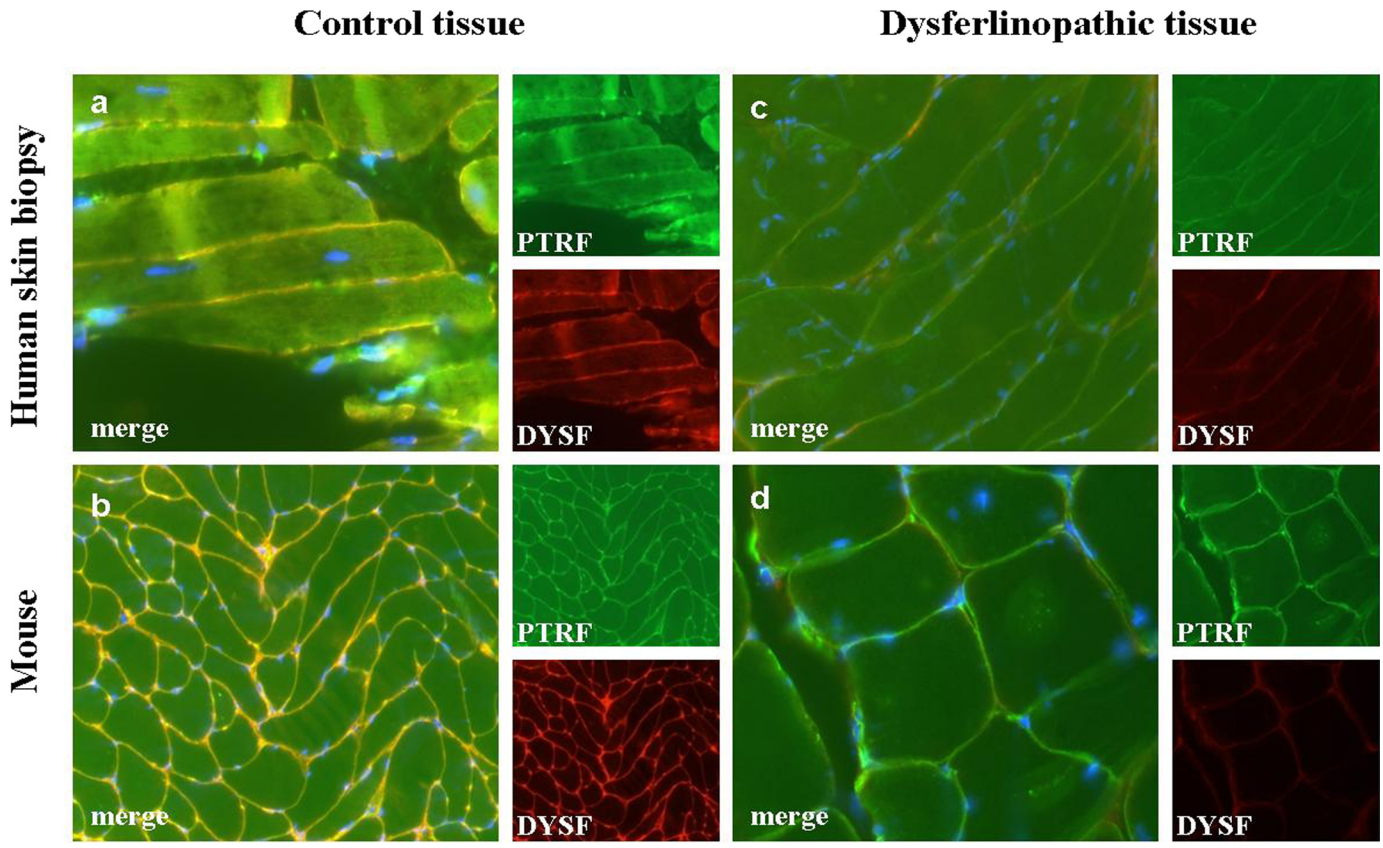

FIGURE 3. **Dysferlin-PTRF co-localization on muscle section.** Dysferlin and PTRF coexpression were tested on (*a*) control human and (*c*) LGMD2B patient skin biopsy (*b*) wt and (*d*) SJL mouse sections using specific antibodies for Dysferlin and PTRF. The results are representative of at least three independent experiments.

cesses such as the cytoskeleton, membrane resealing, sarcomeric structure, enzymatic, and metabolic activity. In addition there are a number of "orphan" LGMD loci, with a map position but no gene identified.

The scope of this report is to obtain data about the common mechanisms underlying muscular dystrophies, which can be caused by mutations at different genetic loci. We used the power of systems biology, through a bioinformatics meta-analysis, since many thousands of microarray experiments are already available and a great deal of information is available. These expression studies provided a lot of information about possible changes occurring in dystrophic tissue, but the any single study is always subject to error. "Reverse-engineering" programs led us to perform a more effective analysis of multiple studies in a single step. With our algorithm we are able to extract the effects of perturbation on the expression of related genes under the control of common factors from the huge amount of data collected in public databases. Co-expressed genes may be co-expressed because of a common regulator. In many biological situations two genes that share a regulator can be anti-correlated, in the sense that while one is activated the other is inhibited from the regulator. The Mutual Information (MI) measures how coherently the expression profiles of two genes vary together, so the MI between two genes is high even though their expression profiles are anti-correlated. The algorithm works when a common factor exists for related functions and this approach can reveal unexpected functional relationships. Albeit the initial aim of the computational analysis we performed was to discover functional related genes and not genes that physically interact, the predicted gene network can still be used to discover such types of interactions (physical and not functional). In this report we used two-dimensional information by combining results from two separate analyses. Starting from a systematic *in silico* analysis of all LGMD-related genes we observed clustering in a functional pathway which gave rise to a huge amount of good quality information. The program utilized clustering to avoid noise due to the different protocols and experiments. Among the different analyses, we focused on Dysferlin and ANHAK, known partners in the membrane resealing apparatus. This approach allowed us to identify a number of potential partners in this pathway.

The Dysferlin query identified a lot of proteins whose expression is confined to inflammatory cells, mainly because of the high expression of Dysferlin in monocytes and the extensive use of blood samples in the assay. It could also reflect the pro-inflammatory state of dysferlinopathy. Among the list of identified genes, CD14 is a surface protein preferentially expressed on monocytes/macrophages. Dysferlin expression in CD14 positive macrophages has been confirmed (32). The AHNAK query identified proteins involved in its protein complex, such as Annexin (A1 and A2) and S100A proteins family. They have been previously described in the literature as involved in the same complex, confirming the power of the algorithm. In agreement with the ubiquitous AHNAK localization at the periphery of the cytoplasm and its function in

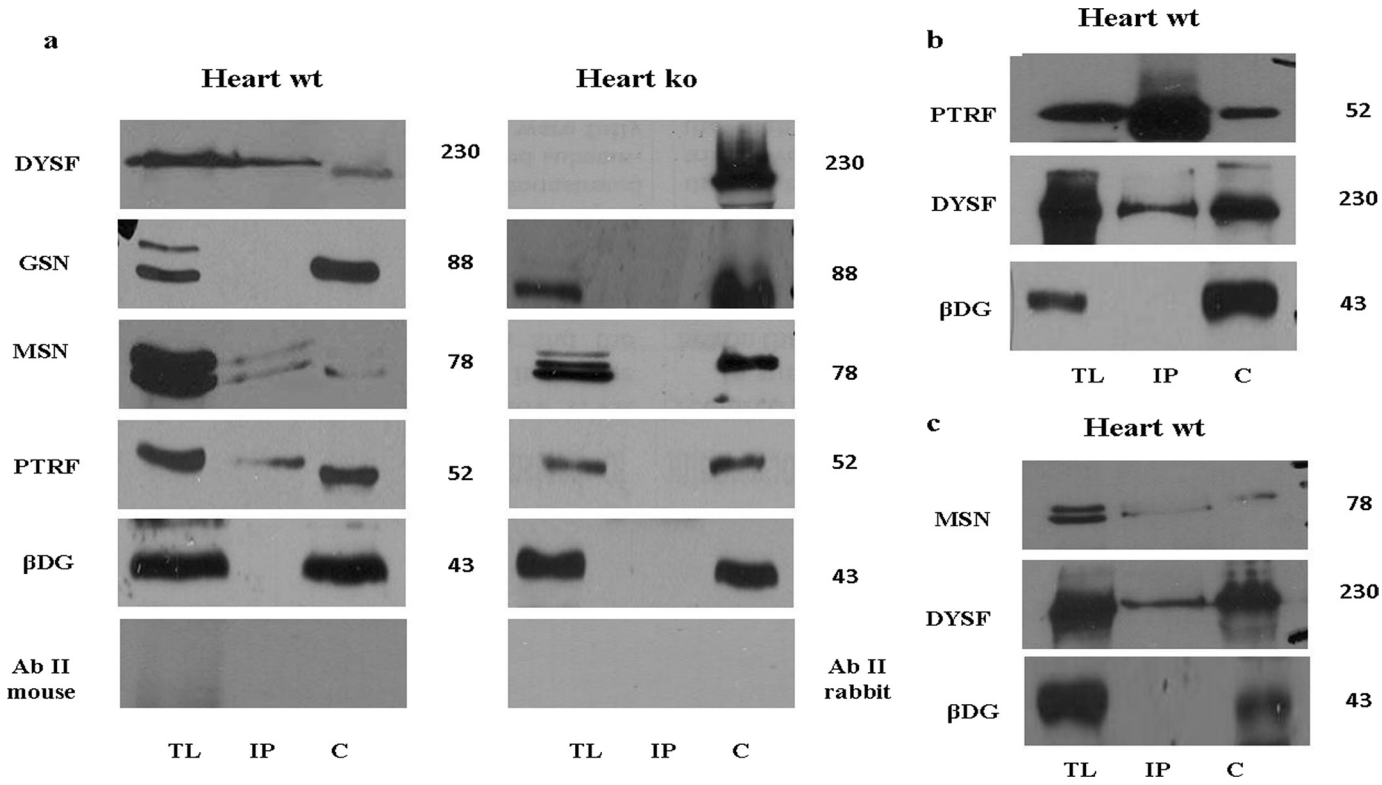

FIGURE 4. **Dysferlin associates with MSN and PTRF *in vivo*.** *a*, heart muscle homogenates from wt and diseased mice were immunoprecipitated with a monoclonal antibody to Dysferlin (*dysf*). Immunoprecipitated complexes were separated on SDS-PAGE gels and immunoblotted. Dysferlin precipitates were blotted forDYSF, MSN, PTRF, GSN, and βDG. Immunoblots were also probed with secondary antibodies alone to exclude nonspecific bands. A muscle lysate from a healthy subject was used as internal positive control. *b* and *c*, BL10 heart muscle homogenates were immunoprecipitated with a polyclonal antibody to PTRF (*b*) and with a monoclonal antibody to MSN (*c*). Immunoprecipitated complexes were separated on SDS-PAGE gels and immunoblotted. PTRF precipitates were blotted for PTRF, DYSF and βDG (*b*). MSN precipitates were blotted for MSN, DYSF, and βDG (*c*). A muscle lysate from a healthy subject was used as internal control. *TL*: total lysate, *IP*: immunoprecipitation, *C*: control. *Black lines* were introduced when more separate gels were used. The results are representative of at least three independent experiments.

cytoskeleton organization and cell membrane cytoarchitecture, the identified genes were all correlated and confirmed an involvement in a common network (see Table 1).

The interaction between AHNAK and Dysferlin in skeletal muscle has been previously described (8). Membership of the same protein complex in skeletal muscle, a primary localization at the sarcolemma and a reduction in muscle from patients with genetically confirmed dysferlinopathy, were all strong evidence to confirm results from the "reverse-engineering" gene network analysis and understand which genes were related to both genes. Cross-referencing the results identified at least 32 genes (Table 2). We focused on GSN, MSN, and PTRF.

Gelsolin (GSN, chr9q33.2) binds to the "plus" ends of actin monomers and filaments to prevent monomer exchange (33). The calcium-regulated protein functions in both assembly and disassembly of actin filaments. Defects in this gene are a cause of familial amyloidosis Finnish type (FAF, Ref. 34). GSN is also a substrate for Calpain 3 cleavage, a protein implicated in the modulation of the Dysferlin/ANHAK complex.

Moesin (for membrane-organizing extension spike protein, MSN, chrXq11.2-q12) is a member of the ERM family that includes ezrin and radixin (35). ERM proteins appear to function as cross-linkers between plasma membranes and actin-based cytoskeletons. It is localized to filopodia and other membranous protrusions that are important for cell-cell recognition and signaling and for cell movement. It has been implicated in vesicle transport.

Polymerase I and transcript release factor (PTRF, chr17q21.2) is a protein that enables the dissociation of paused ternary polymerase I transcription complexes from the 3′-end of pre-rRNA transcripts. It localizes to caveolae at the plasma membrane and is thought to play a critical role in the formation of caveolae and the stabilization of caveolins. Mutations in this gene result in a disorder characterized by generalized lipodystrophy and muscular dystrophy.

Because of their function/localization these gene products were further investigated for their expression in dysferlinopathic tissue, localization and interaction with the Dysferlin protein. We checked these proteins by physical interaction using immunofluorescence, immnoprecipitation, and sedimentation assays. We were able to confirm a relationship between MSN and Dysferlin, and a more intriguing interaction between PTRF and Dysferlin. In combination these assays are indicative of a physical and a functional relation between PTRF and Dysferlin. This is the first time that an interaction between Dysferlin and PTRF has been demonstrated. PTRF was first identified in 1998 (36). However, during the last year, several groups (37–39) showed PTRF (also named Cavin) as an abundant peripheral membrane protein that is resident on the cytoplasmatic face of caveolae. Its distribution coincides with those tissues that express both Cav1 and Cav3. More

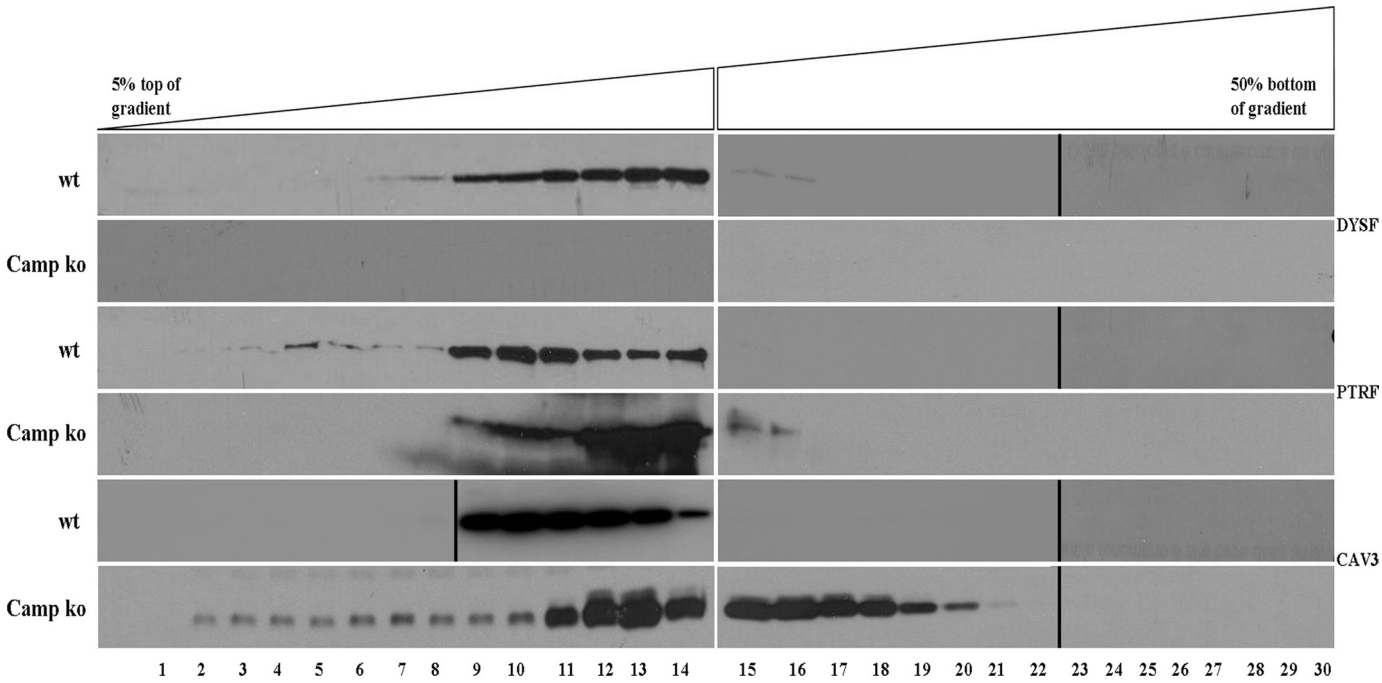

FIGURE 5. **Dysferlin and PTRF co-sedimented into the same fractions.** Skeletal muscles from wild type and diseased (*Camp ko*) mice were collected and homogenized. Intracellular vesicle compartments were isolated by differential centrifugation. Supernatant medium was layered onto a linear 10–50% sucrose-optiprep density gradient and subjected to ultracentrifugation (Sw41Ti rotor, 27,000 rpm for 4 h at 4 °C). Starting from the top of the gradient, fractions were collected and separated on SDS-PAGE gels and then immunobloted with DYSF, Caveolin3 (*CAV3*), and PTRF antibodies to evaluate the relative expression. *Black lines* were introduced when more separate gels were used. The results are representative of at least three independent experiments.

importantly, Cavin-null mice (40, 41) showed a similar phenotype to patients with mutations in PTRF (42, 43): in mice deletion of PTRF causes global loss of caveolae, dyslipidemia, and glucose intolerance. In humans loss of PTRF-Cavin also causes a secondary deficiency of caveolins resulting in muscular dystrophy with generalized lipodystrophy (42, 43). In both reports, the absence of caveolae in muscle fibers leads to a dystrophic phenotype. PRTF and Dysferlin share a common partner in Caveolin-3, the muscle specific caveolin protein family member. Both deficiency of PTRF and Dysferlin cause a reduction of Cav3 staining in muscle fibers. Caveolins are required for Dysferlin trafficking, and caveolin-1 or caveolin-3 mutants cause an accumulation of Dysferlin in the Golgi complex (30). Caveolin-3 and Dysferlin show only a limited co-localization at the sarcolemma in mature muscle fibers and Dysferlin seemed to not be particularly enriched in the caveolae. It has been suggested that the weak association between the two proteins may occur during Dysferlin trafficking, but not at the membrane (44). Dysferlin has been reported to be abnormally localized in LGMD1C (due to mutations in the caveolin-3 gene). Although caveolin-3 deficiency secondarily reduces Dysferlin, the opposite has not been verified. It has been proposed that this may be because Caveolin-3 is more tightly bound to the membrane and does not change when Dysferlin is absent (10, 15, 45). A similar alteration was observed for PTRF: in Dwianingsih *et al.* (46), the authors showed the markedly decreased immunoreactivity for dysferlin at the cell membrane in a PTRF patient, while no alterated staining was evident for PTRF when Dysferlin is mutated (Fig. 3). In keeping with these observations the absence of Dysferlin did not affect the sedimentation of vesicle compartments containing Cav3 and PTRF. Therefore, while Dysferlin requires PTRF and Cav3 for correct localization, the converse is not true. This indicates that PTRF and Cav3 are important in vesicle trafficking, including dysferlin trafficking, but do not depend on dysferlin for their activity. Taken together these data support a functional interaction of CAV3/PTRF/DYSF. Here we characterized the interaction of DYSF with MSN and PTRF in mouse heart lysate and identified two novel putative Dysferlin interacting proteins. Our results could be useful to clarify Dysferlin function in intracellular vesicles and its implication in muscle membrane resealing. With our strategy, we have identified 32 possible candidates for being Dysferlin/ANHAK partners. Additional studies are required to investigate on their role also in monocytes/macrophage. Additional applications of the reverse engineering may shed light on the pathological process of muscular dystrophies, suggesting possible new treatments.

REFERENCES

1. Illa, I., Serrano-Munuera, C., Gallardo, E., Lasa, A., Rojas-García, R., Palmer, J., Gallano, P., Baiget, M., Matsuda, C., and Brown, R. H. (2001) *Ann. Neurol.* **49,** 130–134
2. Bashir, R., Britton, S., Strachan, T., Keers, S., Vafiadaki, E., Lako, M., Richard, I., Marchand, S., Bourg, N., Argov, Z., Sadeh, M., Mahjneh, I., Marconi, G., Passos-Bueno, M. R., Moreira Ede, S., Zatz, M., Beckmann, J. S., and Bushby, K. (1998) *Nat. Genet.* **20,** 37–42
3. Liu, J., Aoki, M., Illa, I., Wu, C., Fardeau, M., Angelini, C., Serrano, C., Urtizberea, J. A., Hentati, F., Hamida, M. B., Bohlega, S., Culper, E. J., Amato, A. A., Bossie, K., Oeltjen, J., Bejaoui, K., McKenna-Yasek, D., Hosler, B. A., Schurr, E., Arahata, K., de Jong, P. J., and Brown, R. H., Jr. (1998) *Nat. Genet.* **20,** 31–36
4. Paradas, C., Llauger, J., Diaz-Manera, J., Rojas-Garcia, R., De Luna, N., Iturriaga, C., Marquez, C., Uson, M., Hankiewicz, K., Gallardo, E., and

Illa, I. (2010) *Neurology* **75,** 316–323
5. Han, R., and Campbell, K. P. (2007) *Curr. Opin. Cell Biol.* **19,** 409–416
6. Bansal, D., and Campbell, K. P. (2004) *Trends Cell Biol.* **14,** 206–213
7. Lennon, N. J., Kho, A., Bacskai, B. J., Perlmutter, S. L., Hyman, B. T., and Brown, R. H., Jr. (2003) *J. Biol. Chem.* **278,** 50466–50473
8. Huang, Y., Laval, S. H., van Remoortere, A., Baudier, J., Benaud, C., Anderson, L. V., Straub, V., Deelder, A., Frants, R. R., den Dunnen, J. T., Bushby, K., and van der Maarel, S. M. (2007) *Faseb. J.* **21,** 732–742
9. Azakir, B. A., Di Fulvio, S., Therrien, C., and Sinnreich, M. (2010) *PloS one* **5,** e10122
10. Matsuda, C., Hayashi, Y. K., Ogawa, M., Aoki, M., Murayama, K., Nishino, I., Nonaka, I., Arahata, K., and Brown, R. H., Jr. (2001) *Hum. Mol. Genet.* **10,** 1761–1766
11. Huang, Y., Verheesen, P., Roussis, A., Frankhuizen, W., Ginjaar, I., Haldane, F., Laval, S., Anderson, L. V., Verrips, T., Frants, R. R., de Haard, H., Bushby, K., den Dunnen, J., and van der Maarel, S. M. (2005) *Eur. J. Hum. Genet.* **13,** 721–730
12. Ampong, B. N., Imamura, M., Matsumiya, T., Yoshida, M., and Takeda, S. (2005) *Acta. Myol.* **24,** 134–144
13. Matsuda, C., Kameyama, K., Tagawa, K., Ogawa, M., Suzuki, A., Yamaji, S., Okamoto, H., Nishino, I., and Hayashi, Y. K. (2005) *J. Neuropathol. Exp. Neurol.* **64,** 334–340
14. Guan, H., and Kiss-Toth, E. (2008) *Adv. Biochem. Eng./Biotechnol.* **110,** 1–24
15. Campanaro, S., Romualdi, C., Fanin, M., Celegato, B., Pacchioni, B., Trevisan, S., Laveder, P., De Pittà, C., Pegoraro, E., Hayashi, Y. K., Valle, G., Angelini, C., and Lanfranchi, G. (2002) *Hum. Mol. Genet.* **11,** 3283–3298
16. von der Hagen, M., Laval, S. H., Cree, L. M., Haldane, F., Pocock, M., Wappler, I., Peters, H., Reitsamer, H. A., Hoger, H., Wiedner, M., Oberndorfer, F., Anderson, L. V., Straub, V., Bittner, R. E., and Bushby, K. M. (2005) *Neuromuscul. Disord.* **15,** 863–877
17. Walker, W. L., Liao, I. H., Gilbert, D. L., Wong, B., Pollard, K. S., McCulloch, C. E., Lit, L., and Sharp, F. R. (2008) *BMC Genomics* **9,** 494
18. Celegato, B., Capitanio, D., Pescatori, M., Romualdi, C., Pacchioni, B., Cagnin, S., Viganò, A., Colantoni, L., Begum, S., Ricci, E., Wait, R., Lanfranchi, G., and Gelfi, C. (2006) *Proteomics* **6,** 5303–5321
19. Parkinson, H., Kapushesky, M., Kolesnikov, N., Rustici, G., Shojatalab, M., Abeygunawardena, N., Berube, H., Dylag, M., Emam, I., Farne, A., Holloway, E., Lukk, M., Malone, J., Mani, R., Pilicheva, E., Rayner, T. F., Rezwan, F., Sharma, A., Williams, E., Bradley, X. Z., Adamusiak, T., Brandizi, M., Burdett, T., Coulson, R., Krestyaninova, M., Kurnosov, P., Maguire, E., Neogi, S. G., Rocca-Serra, P., Sansone, S. A., Sklyar, N., Zhao, M., Sarkans, U., and Brazma, A. (2009) *Nucleic Acids Res.* **37,** D868–D872
20. Butte, A. J., and Kohane, I. S. (2000) *Pacific Symposium on Biocomputing* 418–429
21. Linding, R., Jensen, L. J., Ostheimer, G. J., van Vugt, M. A., Jørgensen, C., Miron, I. M., Diella, F., Colwill, K., Taylor, L., Elder, K., Metalnikov, P., Nguyen, V., Pasculescu, A., Jin, J., Park, J. G., Samson, L. D., Woodgett, J. R., Russell, R. B., Bork, P., Yaffe, M. B., and Pawson, T. (2007) *Cell* **129,** 1415–1426
22. Margolin, A. A., Nemenman, I., Basso, K., Wiggins, C., Stolovitzky, G., Dalla Favera, R., and Califano, A. (2006) *BMC Bioinformatics* **7,** Suppl. 1, S7
23. Bittner, R. E., Anderson, L. V., Burkhardt, E., Bashir, R., Vafiadaki, E., Ivanova, S., Raffelsberger, T., Maerk, I., Höger, H., Jung, M., Karbasiyan, M., Storch, M., Lassmann, H., Moss, J. A., Davison, K., Harrison, R., Bushby, K. M., and Reis, A. (1999) *Nat. Genet.* **23,** 141–142
24. Bansal, D., Miyake, K., Vogel, S. S., Groh, S., Chen, C. C., Williamson, R., McNeil, P. L., and Campbell, K. P. (2003) *Nature* **423,** 168–172
25. Klinge, L., Laval, S., Keers, S., Haldane, F., Straub, V., Barresi, R., and Bushby, K. (2007) *Faseb J* **21,** 1768–1776
26. Santoro, L., Nolano, M., Faraso, S., Fiorillo, C., Vitiello, C., Provitera, V., Aurino, S., and Nigro, V. (2010) *Muscle Nerve* **41,** 392–398
27. Sardiello, M., Palmieri, M., di Ronza, A., Medina, D. L., Valenza, M., Gennarino, V. A., Di Malta, C., Donaudy, F., Embrione, V., Polishchuk, R. S., Banfi, S., Parenti, G., Cattaneo, E., and Ballabio, A. (2009) *Science* **325,** 473–477
28. Hill, M. M., Bastiani, M., Luetterforst, R., Kirkham, M., Kirkham, A., Nixon, S. J., Walser, P., Abankwa, D., Oorschot, V. M., Martin, S., Hancock, J. F., and Parton, R. G. (2008) *Cell* **132,** 113–124
29. Cai, C., Weisleder, N., Ko, J. K., Komazaki, S., Sunada, Y., Nishi, M., Takeshima, H., and Ma, J. (2009) *J. Biol. Chem.* **284,** 15894–15902
30. Hernández-Deviez, D. J., Howes, M. T., Laval, S. H., Bushby, K., Hancock, J. F., and Parton, R. G. (2008) *J. Biol. Chem.* **283,** 6476–6488
31. Nigro, V. (2003) *Acta. Myol.* **22,** 35–42
32. de Luna, N., Gallardo, E., Soriano, M., Dominguez-Perles, R., de la Torre, C., Rojas-García, R., García-Verdugo, J. M., and Illa, I. (2006) *J. Biol. Chem.* **281,** 17092–17098
33. Sun, H. Q., Yamamoto, M., Mejillano, M., and Yin, H. L. (1999) *J. Biol. Chem.* **274,** 33179–33182
34. Burtnick, L. D., Urosev, D., Irobi, E., Narayan, K., and Robinson, R. C. (2004) *EMBO J.* **23,** 2713–2722
35. Lankes, W. T., and Furthmayr, H. (1991) *Proc. Natl. Acad. Sci. U. S. A.* **88,** 8297–8301
36. Jansa, P., Mason, S. W., Hoffmann-Rohrer, U., and Grummt, I. (1998) *EMBO J.* **17,** 2855–2864
37. Aboulaich, N., Vainonen, J. P., Stralfors, P., and Vener, A. V. (2004) *Biochem. J.* **383,** 237–248
38. Pilch, P. F., Souto, R. P., Liu, L., Jedrychowski, M. P., Berg, E. A., Costello, C. E., and Gygi, S. P. (2007) *J. Lipid Res.* **48,** 2103–2111
39. Vinten, J., Johnsen, A. H., Roepstorff, P., Harpøth, J., and Tranum-Jensen, J. (2005) *Biochim. Biophys. Acta* **1717,** 34–40
40. Liu, L., Brown, D., McKee, M., Lebrasseur, N. K., Yang, D., Albrecht, K. H., Ravid, K., and Pilch, P. F. (2008) *Cell Metab.* **8,** 310–317
41. Liu, L., and Pilch, P. F. (2008) *J. Biol. Chem.* **283,** 4314–4322
42. Hayashi, Y. K., Matsuda, C., Ogawa, M., Goto, K., Tominaga, K., Mitsuhashi, S., Park, Y. E., Nonaka, I., Hino-Fukuyo, N., Haginoya, K., Sugano, H., and Nishino, I. (2009) *J. Clin. Investig.* **119,** 2623–2633
43. Rajab, A., Straub, V., McCann, L. J., Seelow, D., Varon, R., Barresi, R., Schulze, A., Lucke, B., Lützkendorf, S., Karbasiyan, M., Bachmann, S., Spuler, S., and Schuelke, M. (2010) *PLoS. Genet.* **6,** e1000874
44. Hernández-Deviez, D. J., Martin, S., Laval, S. H., Lo, H. P., Cooper, S. T., North, K. N., Bushby, K., and Parton, R. G. (2006) *Human Mol. Genet.* **15,** 129–142
45. Walter, M. C., Braun, C., Vorgerd, M., Poppe, M., Thirion, C., Schmidt, C., Schreiber, H., Knirsch, U. I., Brummer, D., Müller-Felber, W., Pongratz, D., Müller-Höcker, J., Huebner, A., and Lochmüller, H. (2003) *J. Neurol.* **250,** 1431–1438
46. Dwianingsih, E. K., Takeshima, Y., Itoh, K., Yamauchi, Y., Awano, H., Malueka, R. G., Nishida, A., Ota, M., Yagi, M., and Matsuo, M. (2010) *Mol. Genet. Metab.* **101,** 233–237